

Cerebral amyloid burden is associated with white matter hyperintensity location in specific posterior white matter regions

Nick A. Weaver^{a,*}, Thomas Doeven^a, Frederik Barkhof^{b,c}, J. Matthijs Biesbroek^a, Onno N. Groeneveld^a, Hugo J. Kuijf^d, Niels D. Prins^{e,f}, Philip Scheltens^f, Charlotte E. Teunissen^g, Wiesje M. van der Flier^{f,h}, Geert Jan Biessels^a, on behalf of the TRACE-VCI study group

^a Department of Neurology and Neurosurgery, UMC Utrecht Brain Center, University Medical Center Utrecht, the Netherlands

^b Institutes of Neurology and Healthcare Engineering, UCL, London, UK

^c Department of Radiology and Nuclear Medicine, Amsterdam Neuroscience, Vrije Universiteit Amsterdam, Amsterdam UMC, Amsterdam, the Netherlands

^d Image Sciences Institute, University Medical Center Utrecht, Utrecht, the Netherlands

^e Brain Research Center, Amsterdam, the Netherlands

^f Alzheimer Center Amsterdam, Department of Neurology, Amsterdam Neuroscience, Vrije Universiteit Amsterdam, Amsterdam UMC, Amsterdam, the Netherlands

^g Neurochemistry Lab and Biobank, Department of Clinical Chemistry, Amsterdam Neuroscience, VU University Medical Center Amsterdam, Amsterdam, the Netherlands

^h Department of Epidemiology and Biostatistics, Amsterdam Neuroscience, Vrije Universiteit Amsterdam, Amsterdam UMC, Amsterdam, the Netherlands

ARTICLE INFO

Article history:

Received 19 April 2019

Received in revised form 2 August 2019

Accepted 3 August 2019

Keywords:

Alzheimer's disease

Cerebrospinal fluid

Amyloid-beta

Tau

White matter hyperintensities

Magnetic resonance imaging

Lesion mapping

ABSTRACT

White matter hyperintensities (WMHs) are a common manifestation of cerebral small vessel disease. WMHs are also frequently observed in patients with familial and sporadic Alzheimer's disease, often with a particular posterior predominance. Whether amyloid and tau pathologies are linked to WMH occurrence is still debated. We examined whether cerebral amyloid and tau burden, reflected in cerebrospinal fluid amyloid-beta 1-42 (A β -42) and phosphorylated tau (p-tau), are related to WMH location in a cohort of 517 memory clinic patients. Two lesion mapping techniques were performed: voxel-based analyses and region of interest-based linear regression. Voxelwise associations were found between lower A β -42 and parieto-occipital periventricular WMHs. Regression analyses demonstrated that lower A β -42 correlated with larger WMH volumes in the splenium of the corpus callosum and posterior thalamic radiation, also after controlling for markers of vascular disease. P-tau was not consistently related to WMH occurrence. Our findings indicate that cerebral amyloid burden is associated with WMHs located in specific posterior white matter regions, possibly reflecting region-specific effects of amyloid pathology on the white matter.

© 2019 The Authors. Published by Elsevier Inc. This is an open access article under the CC BY license

(<http://creativecommons.org/licenses/by/4.0/>).

1. Introduction

White matter hyperintensities (WMHs) are a common radiological finding in older subjects and in patients with dementia (Gorelick et al., 2011). In this context, WMHs are often considered to primarily represent ischemic damage caused by cerebral small vessel disease

(SVD) (Pantoni, 2010; Wardlaw et al., 2015). There are also clear indications for a relationship between WMHs and Alzheimer's disease (AD) (Brickman, 2013). WMH burden predicts the clinical risk of AD (Brickman et al., 2012; Lindemer et al., 2015; Prins et al., 2004; Smith et al., 2008; Vermeer et al., 2003; Wolf et al., 2000), and WMHs are more prevalent and severe in patients diagnosed with AD compared with nondemented elderly (Kalaria, 2000; Rezek et al., 1987; Scheltens et al., 1992). Of note, increased WMH volume is an early imaging feature in monogenic hereditary forms of AD, particularly in presenilin 1 (PSEN1), presenilin 2 (PSEN2), and amyloid precursor protein (APP) mutation carriers, also at an age at which "normal" aging-related WMHs are still uncommon (Lee et al., 2016).

* Corresponding author at: Department of Neurology, University Medical Center Utrecht, Heidelberglaan 100, Internal mail no. G03.124, 3508, GA Utrecht, the Netherlands. Tel.: +31 88 7556866; fax: +31 30 2542100.

E-mail address: n.a.weaver@umcutrecht.nl (N.A. Weaver).

The nature of the relationship between WMHs and AD is still under debate. From an etiological perspective, this debate centers on the question whether WMHs and AD pathologies should be regarded as independent processes with additive effects on dementia risk, or whether one contributes to the other (Koncz and Sachdev, 2018). Current biological models suggest involvement of cerebral SVD in pathways that lead to the accumulation of cerebral amyloid and tau (Kisler et al., 2017). Further indications that amyloid-related processes and WMHs are interrelated comes from recent studies that show that lower cerebrospinal fluid (CSF) amyloid-beta 1–42 (A β -42) levels—reflective of a higher amyloid burden in the brain (Blennow et al., 2015; Molinuevo et al., 2018)—are associated with larger WMH volumes in patients with sporadic AD (Osborn et al., 2018; Pietroboni et al., 2018; Shams et al., 2016; Van Westen et al., 2016), mild cognitive impairment (MCI) (Osborn et al., 2018), and cognitively healthy individuals (Kandel et al., 2016; Marnane et al., 2016; Pietroboni et al., 2018; Scott et al., 2016). By contrast, studies on the relationship between WMH burden and CSF p-tau are scarce and provide conflicting results (Hertze et al., 2013; Marnane et al., 2016).

In the context of AD, WMHs may have particular spatial features, which is particularly evident in patients with rare genetic forms of AD. For example, in PSEN1 mutation carriers, WMHs can extend into the subcortical U-fibers (Ryan et al., 2015), while this location is typically spared in SVD-related WMHs (Chao et al., 2006). In PSEN1, PSEN2, and APP mutation carriers, parietal and occipital WMHs are an early imaging feature that occurs around the same time as early changes in CSF A β -42 (Lee et al., 2016). WMHs also show a posterior predominance in patients with sporadic AD (Yoshita et al., 2006) and cerebral amyloid angiopathy (CAA) (Thanprasertsuk et al., 2014; Zhu et al., 2012). This posterior WMH distribution pattern stands in contrast to the frontotemporal predominance of WMH that is seen in patients with cerebral autosomal dominant arteriopathy with subcortical infarcts and leukoencephalopathy, which is considered a model of pure cerebral SVD (Auer et al., 2001; Singhal et al., 2005).

These observations raise the question whether amyloid pathology itself, as pathological hallmark of AD, is linked to WMH occurrence in specific white matter regions. Modern “lesion mapping” techniques can determine the relationship between brain lesion location and clinical measures at very high spatial resolution (de Haan and Karnath, 2017). One recent study found associations between lower CSF A β -42 levels and WMHs located in the posterior corona radiata in individuals with normal cognition or MCI (Al-Janabi et al., 2018). However, these findings were restricted by limited lesion coverage in the brain, and limited statistical power for voxelwise analyses, both related to the small sample size ($n = 62$) (Al-Janabi et al., 2018). Importantly, subjects with dementia were excluded, thus the relationship between amyloid and WMH location in individuals at more severe disease stages remains unclear. These limitations can be overcome by applying lesion mapping techniques on a much larger cohort—preferably with hundreds of subjects (Weaver et al., 2019)—with individuals across the full spectrum of clinical disease stages.

In the present study, we aimed to determine whether cerebral amyloid burden relates to specific WMH locations using lesion mapping approaches. For this purpose, we selected a large memory clinic population with available CSF biomarkers for AD pathology and manifestations of vascular brain injury on magnetic resonance imaging (MRI), including WMHs. We studied the relation between CSF A β -42 and WMH location on MRI using voxel-based and region of interest-based lesion mapping analyses. We hypothesized that lower CSF A β -42 levels would be associated with WMHs located in posterior white matter regions. As secondary objective, we explored whether CSF measures of phosphorylated tau (p-tau) are related to WMH location, using the same lesion-mapping

approaches. As the second core biomarker of AD, phosphorylated tau could—alternatively or concurrently with A β -42—be related to particular WMH locations.

2. Methods

2.1. TRACE-VCI cohort

Patients were selected from the TRACE-VCI study cohort (Utrecht-Amsterdam clinical features and prognosis in Vascular Cognitive Impairment), which consists of 860 memory clinic patients from Dutch outpatient clinics at two university hospitals (Amsterdam UMC location VUMC and University Medical Center Utrecht [UMCU]). Detailed inclusion and exclusion criteria were previously described (Boomsma et al., 2017). In short, patients were eligible for inclusion if they showed at least a minimal burden of vascular brain injury on MRI, meaning that either WMHs or other vascular brain lesions such as infarcts or hemorrhages were present. Co-occurrence of neurodegenerative disorders and depression, together with this vascular injury, was accepted, in line with proposed criteria for possible vascular cognitive impairment (O'Brien et al., 2003). Patients with primary nonvascular and non-degenerative causes of cognitive dysfunction or psychiatric disease other than depression were excluded. Patients with monogenic vascular or nonvascular causes of cognitive impairment (e.g., NOTCH3 mutations) were also excluded. All patients first visited the memory clinic between September 2009 and December 2013 and underwent a standardized one-day memory clinic evaluation, consisting of an interview, physical and neurological examination, laboratory testing, neuropsychological assessment, and brain MRI. Clinical diagnoses were established at multidisciplinary consensus meetings using internationally established diagnostic criteria, without knowledge of CSF biomarkers or APOE genotyping (Boomsma et al., 2017).

The study was approved by the institutional review board of the VUMC and the UMCU. All patients provided informed consent before research related procedures.

2.2. Study sample

A flowchart of patient selection for present study is presented in Fig. 1. Thirty-seven patients were excluded during preprocessing of imaging data, mostly because of MRI data were not available or of insufficient quality, or if technical errors occurred during data processing. One additional patient was excluded because of failed lesion registration. Finally, 305 patients were excluded because CSF biomarkers were not available. This resulted in the final study sample of 517 patients.

2.3. Imaging protocol

The MRI protocol of the TRACE-VCI study is described extensively elsewhere (Boomsma et al., 2017). In short, brain MRI scans were made using 1.5 tesla ($n = 29$; 5.6%) or 3.0 tesla ($n = 488$; 94.4%) MRI scanners. The standardized scanning protocol consisted of 3D T1-weighted, 2D T2-weighted, 2D T2*-weighted or susceptibility-weighted imaging, and 2D or 3D fluid-attenuated inversion recovery sequences.

2.4. Lesion segmentation

Lesion segmentation was performed on fluid-attenuated inversion recovery sequences, using T1 as an anatomical reference for proper lesion classification. Cerebrovascular lesions were rated in accordance with the internationally established STRIVE

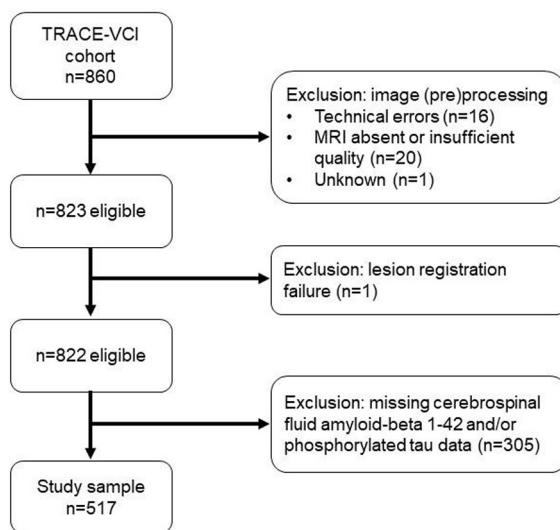


Fig. 1. Flowchart of study sample selection.

criteria, which provide neuroimaging standards for classification of cerebral small vessel disease (Wardlaw et al., 2013). Automated WMH segmentation was performed using the k-nearest neighbor classification with tissue type priors method. This method has shown excellent performance for different scanners and patient populations (Steenwijk et al., 2013). The resulting WMH segmentations underwent a visual check for accuracy by two independent raters (NAW and TD). Manual corrections were performed in 6 subjects (<1% of the TRACE-VCI cohort) when important inaccuracies were found, such as missed WMHs, or incorrect or incomplete WMH segmentation. Presence of other lesion types (e.g., lacunar infarcts, nonlacunar infarcts, and hemorrhages) was rated visually by neuroradiologists. Manual segmentation of these lesions was performed with in-house developed software using MeVisLab (MeVis Medical Solutions AG, Bremen, Germany) (Ritter et al., 2011).

2.5. Generation of lesion maps

The RegLSM image-processing pipeline (publicly available at www.metavcimap.org (most recent version described in [Weaver et al., 2019])) was used to transform all lesion maps to the T1 1-mm MNI-152 (Montreal Neurological Institute) brain template (Fonov et al., 2011). The registration procedure consisted of linear registration followed by nonlinear registration, using the elastix toolbox (Klein et al., 2010). As an intermediate step, registration to an age-specific MRI template was performed (Rorden et al., 2012), which provides a more accurate registration in cases of severe brain atrophy. These registration steps were combined into a single step in which the original lesion maps were registered directly to MNI-152 space, to prevent intermediate interpolations and thereby improve registration accuracy. Quality checks of all registration results were performed by one rater (NAW). One patient (0.14%) was ultimately excluded because of unsuccessful lesion registration. As final step, voxels that were also labeled as other lesions were discarded from the WMH lesion maps, to prevent that hyperintense signals resulting from such lesions (e.g., gliotic scar tissue from infarcts or hemorrhages) would be misclassified as WMHs. This allowed us to create reliable WMH lesion maps even when other lesions, such as infarcts or hemorrhages, were present on MRI.

2.6. Cerebrospinal fluid biomarkers

CSF concentrations of A β -42 and phosphorylated tau at threonine 181 (p-tau) were measured at the Neurochemistry laboratory at the Department of Clinical Chemistry of the VUMC (Mulder et al., 2010). CSF biomarkers were assessed using Sandwich ELISAs (Fujirebio, Ghent, Belgium) (Lewczuk et al., 2006). CSF was obtained from patients at the VUMC as part of the clinical workup (76.8% of TRACE-VCI VUMC subjects), and less frequently at the UMCU (16.3%). Two measures for CSF biomarker burden were used: CSF levels as continuous measure, and the presence or absence of CSF abnormality based on validated cutoff scores of <640 ng/L for A β -42 (Zwan et al., 2014) and >52 ng/L for p-tau (Mulder et al., 2010). Because p-tau is considered a more specific marker of AD pathology than total tau (Blennow et al., 2010), total tau was not assessed in this study.

2.7. Statistical analysis

IBM SPSS Statistics for Windows (Released 2016, Version 24.0, Armonk, NY: IBM Corp) was used for statistical analyses unless otherwise indicated. Differences between included and excluded patients from the TRACE-VCI cohort were assessed using independent sample t-tests, Mann-Whitney U tests or Pearson's χ^2 tests where appropriate.

Two assumption-free analysis methods were used to assess the relation between CSF biomarker levels and WMH location: voxel-based lesion symptom mapping (VLSM), to determine the relation between CSF biomarker levels and presence of WMHs for individual voxels in the brain; and region of interest (ROI)-based analyses, to analyze the relation between CSF biomarker levels and regional WMH volumes in predefined white matter regions. Each method has a different modeling approach, thereby providing complementary information on WMH location. VLSM offers higher spatial resolution, at the cost of statistical power due to control for multiple comparisons. Meanwhile, ROI-based analyses can take cumulative lesion burden in particular brain regions into account. CSF biomarker levels as continuous measure were analyzed in both lesion mapping methods. The dichotomous measure for presence or absence of CSF abnormality was used in the ROI-based analyses but not for VLSM. Dichotomization leads to a significant loss of statistical power, and VLSM with dichotomized data was not expected to survive the strict correction for multiple testing.

2.7.1. Voxel-based lesion-symptom mapping

VLSM was performed using the Non-Parametric Mapping software (version May 2016; settings: univariate analysis, Brunner-Munzel test) (Rorden et al., 2007). Z-scores for CSF A β -42 and p-tau levels were used, after correction for age and sex. Next, to determine whether voxelwise associations were independent of global WMH burden, the analyses were repeated after additional correction for normalized total WMH volume (i.e., volumes calculated from lesion maps in MNI-152 space) and a vascular risk summary score. This score reflects the number of vascular risk factors that is present, from a total of six (diabetes mellitus, hypertension, hypercholesterolemia, smoking, obesity, and history of vascular events other than stroke), similar to a previous study (Lee et al., 2016). Presence of these risk factors was based on medical history and/or medication use and for hypertension or diabetes also based on results from clinical and laboratory testing at the baseline assessment. Further details were previously described (Boomsma et al., 2017). Voxels affected in less than 10 (2%) patients were excluded from the analyses. False discovery rate control ($q < 0.05$) was applied to correct for multiple comparisons.

2.7.2. Region of interest-based analysis

Regional WMH volumes were calculated (in milliliters) using the ICBM-DTI-81 white matter atlas in MNI-152 space (Mori et al., 2008; Oishi et al., 2008). Because we had no a priori hypotheses about laterality, bilateral regions were merged to create a single ROI by combining the left and right volumes to reduce the number of comparisons. ROIs that were affected by WMHs in less than 25 patients were excluded. WMH volumes underwent cube root transformation to meet the normality assumptions of multiple linear models.

Total and regional WMH volumes were entered as dependent variables in the linear regression models. First, age and sex were entered as independent variables into a model for each ROI separately (model 1). Next, CSF A β -42 and p-tau levels as continuous measures (model 2) and the presence of CSF abnormality (model 3) were independently added to the initial model. Standardized betas ($\text{std}\beta$) and explained variances (adjusted R²) of each model were calculated. Bonferroni correction for multiple comparisons was applied (i.e., 16 comparisons, $p < 0.0031$).

Several supplementary analyses were performed. First, to explore whether the associations differed between clinical diagnoses (i.e., subjective cognitive decline [SCD], MCI, AD-type dementia, and non-AD-type dementia), interaction terms (dummy-diagnosis*CSF measure) were added to the model if a significant association between a CSF biomarker and regional WMH volumes

was found. Subsequently, when this interaction term was significant ($p < 0.05$), regression analyses were stratified for clinical diagnosis, and standardized betas were calculated for each diagnostic subgroup separately. Second, we repeated the ROI-based analyses in a subgroup of patients with biologically defined AD. This subgroup was selected based on the concurrent presence of CSF A β -42 and p-tau abnormality (cutoffs defined in section 2.6), following the AT(N) criteria for AD (Jack et al., 2018). Finally, the analyses on CSF A β -42 were additionally adjusted for vascular risk factors and for presence of strictly lobar cerebral microbleeds as markers for arteriosclerosis and CAA, respectively, in a subgroup of 491 patients. Vascular risk factors were added to the model in two forms: as a vascular risk summary score (described in section 2.7.1), and also as separate factors to determine their individual contribution in the ROI-based analyses. Presence of one or more strictly lobar cerebral microbleeds was taken as indicator of “possible CAA” in accordance with the modified Boston criteria (Linn et al., 2010).

3. Results

3.1. Demographic and clinical characteristics

Demographic and clinical characteristics of the present study sample are shown in Table 1. The mean age was 66.8 years, and 237

Table 1
Demographic and clinical characteristics of the study sample

Characteristics	Study sample (n = 517)	SCD (n = 121)	MCI (n = 118)	AD (n = 184)	Other dementia (n = 94)
Demographic characteristics					
Age, mean \pm SD	66.8 \pm 7.6	63.5 \pm 7.5	68.0 \pm 7.4	68.5 \pm 7.6	66.4 \pm 6.7
Female, n (%)	237 (45.8)	56 (46.3)	47 (39.8)	97 (52.7)	37 (39.4)
Education (Verhage scale) ^a , median (IQR)	5 (2) (n = 512) ^b	5 (2)	5 (2) (n = 115) ^b	5 (2) (n = 183) ^b	5 (2) (n = 93) ^b
Vascular risk factors					
Diabetes mellitus, n (%)	79 (15.3)	12 (9.9)	26 (22.0)	27 (14.7)	14 (14.9)
Hypertension, n (%)	421 (81.4)	94 (77.7)	94 (79.7)	154 (83.7)	79 (84.0)
Hypercholesterolemia, n (%)	208 (40.2)	42 (34.7)	58 (49.2)	75 (40.8)	33 (35.1)
Current smoker, n (%)	106 (20.5) (n = 513) ^b	24 (20.0) (n = 120) ^b	25 (21.2)	37 (20.3) (n = 182) ^b	93 (21.5) (n = 93) ^b
Obesity (BMI \geq 30), n (%)	95 (18.4) (n = 509) ^b	32 (26.4)	13 (11.2) (n = 117) ^b	29 (16.1) (n = 180) ^b	21 (22.8) (n = 92) ^b
History of reported stroke, n (%)	23 (4.4)	6 (5.0)	8 (6.8)	3 (1.6)	6 (6.4)
History of vascular event other than stroke, n (%)	43 (8.3)	5 (4.1)	13 (11.0)	15 (8.2)	10 (10.6)
Cerebrospinal fluid AD biomarkers					
CSF A β -42 (ng/L), median (IQR)	618 (466)	916 (342)	628 (445)	476 (172)	822 (456)
CSF p-tau (ng/L), median (IQR)	56 (43)	47 (24)	60 (40)	75 (52)	39 (28)
CSF A β -42 abnormal at cutoff <640 ng/L, n (%)	271 (52.4)	24 (19.8)	61 (51.7)	157 (85.3)	29 (30.9)
CSF p-tau abnormal at cutoff >52 ng/L, n (%)	279 (54.0)	44 (36.4)	68 (57.6)	137 (74.5)	30 (31.9)
Cognitive characteristics					
Mini-Mental State Examination, median (IQR)	25 (7) (n = 515) ^b	28 (2)	27 (3)	20 (7)	24 (6) (n = 92) ^b
Clinical Dementia Rating, median (IQR)	0.5 (0.5)	0 (0.5)	0.5 (0)	1.0 (0.5)	0.5 (0.5)
Imaging characteristics					
WMH volume in milliliters ^c , median (IQR)	9.0 (16.6)	4.9 (8.9)	11.6 (17.7)	11.6 (19.3)	8.5 (23.0)
Patients with at least one lacune, n (%)	81 (15.7) (n = 505) ^b	10 (8.3) (n = 119) ^b	26 (23.2) (n = 112) ^b	22 (12.2) (n = 181) ^b	23 (24.7) (n = 93) ^b
Patients with at least one strictly lobar microbleed, n (%)	153 (31.2) (n = 491) ^b	36 (31.6) (n = 114) ^b	30 (26.1) (n = 115) ^b	62 (35.6) (n = 174) ^b	25 (28.4) (n = 88) ^b
Patients with cortical brain infarct, n (%)	33 (6.4)	3 (2.5)	5 (4.2)	7 (3.8)	7 (7.4)
Patients with intracranial hemorrhage, n (%)	3 (0.6)	0 (0.0)	1 (0.8)	2 (1.1)	0 (0.0)

Key: AD, Alzheimer's disease; A β -42, amyloid-beta 1-42; BMI, body mass index; CSF, cerebrospinal fluid; IQR, interquartile range; MCI, mild cognitive impairment; p-tau, phosphorylated tau at threonine 181; SCD, subjective cognitive decline; SD, standard deviation; WMH, white matter hyperintensity.

^a Verhage scale: 1 = <6 y of primary education; 2 = finished 6 y of primary education; 3 = 6 y primary education and <2 y of low level secondary education; 4 = 4 y of low level secondary education; 5 = 4 y of average level secondary education; 6 = 5 y of high level secondary education; 7 = university degree (Verhage, 1964).

^b Missing data; available sample size (n) is noted behind the respective variable.

^c Standardized WMH volumes were calculated from lesion maps after transformation to the MNI-152 brain template.

patients (46%) were women. 121 patients (23.4%) had a clinical diagnosis of SCD, 118 patients (22.8%) had MCI, 184 patients (35.6%) had AD type dementia, and 94 patients (18.2%) had other types of dementia (vascular dementia: $n = 19$; frontotemporal dementia: $n = 20$; Lewy body dementia: $n = 13$; other or unknown etiology: $n = 42$). 196 patients (37.9%) were amyloid- and tau-positive, thereby fulfilling the criteria for biologically defined AD (Jack et al., 2018). WMHs were present in all included patients; there was substantial variation in the number of voxels affected, with a right-skewed distribution across the study sample (normalized total WMH volumes: median: 9.0 mL, IQR: 16.6 mL, 5th percentile: 1.4 mL, 95th percentile: 57.5 mL).

Characteristics stratified by diagnostic group are also presented. Of note, total WMH volumes were higher in patients with MCI and dementia compared with SCD. CSF A β -42 levels were lowest in patients with AD type dementia, followed by patients with MCI. CSF p-tau levels were highest in patients with AD type dementia, followed by patients with MCI. CSF A β -42 and p-tau abnormalities were present in most patients with AD type dementia (85.3% and 74.5%, respectively), and also to a large extent in other diagnostic groups (20%–58%).

The vascular risk summary score showed weak correlations with CSF A β -42, CSF p-tau, and total WMH volume (Spearman's coefficient: 0.117, 0.142 and -0.088, respectively). Individual vascular risk factors were not related to significant differences in total WMH volume, lower A β -42 levels or higher p-tau levels (data not shown). Compared with the excluded TRACE-VCI subjects, the selected study sample was younger, had lower WMH burden, and had lower

prevalence of vascular risk factors and cerebrovascular lesions on MRI (Supplementary Table 1).

3.2. Spatial distribution of WMHs

The spatial distribution of WMHs is shown in Fig. 2A. WMHs had a symmetrical distribution, with most lesions located in periventricular and frontoparietal regions. 26% of the white matter on the MNI-152 template (153,626 of 596,258 voxels; including brain stem and cerebellum) was affected in at least 10 subjects, and could therefore be included in the VLSM analyses. For the ROI-based analyses, 16 white matter regions were affected in sufficient number of patients to be included (Tables 2 and 3). Regional WMH volumes per ROI are shown in Supplementary Table 2.

3.3. Relation between A β -42 and WMHs

Overall, lower CSF A β -42 levels correlated with larger total WMH volume ($\text{std}\beta = -0.131, p = 0.002$) (Table 2). VLSM identified voxels in bilateral parieto-occipital periventricular regions, where lower CSF A β -42 levels, that is, reflecting a higher load of cerebral amyloid pathology (Blennow et al., 2015; Molinuevo et al., 2018), were related to prevalence of WMH, after correction for age, sex, and multiple comparisons (Fig. 2B). Multiple-voxel clusters within these regions remained significant after additional correction for total WMH volume and the vascular risk summary score.

In the ROI-based analyses, lower CSF A β -42 levels (continuous measure) and the presence of CSF A β -42 abnormality (dichotomous

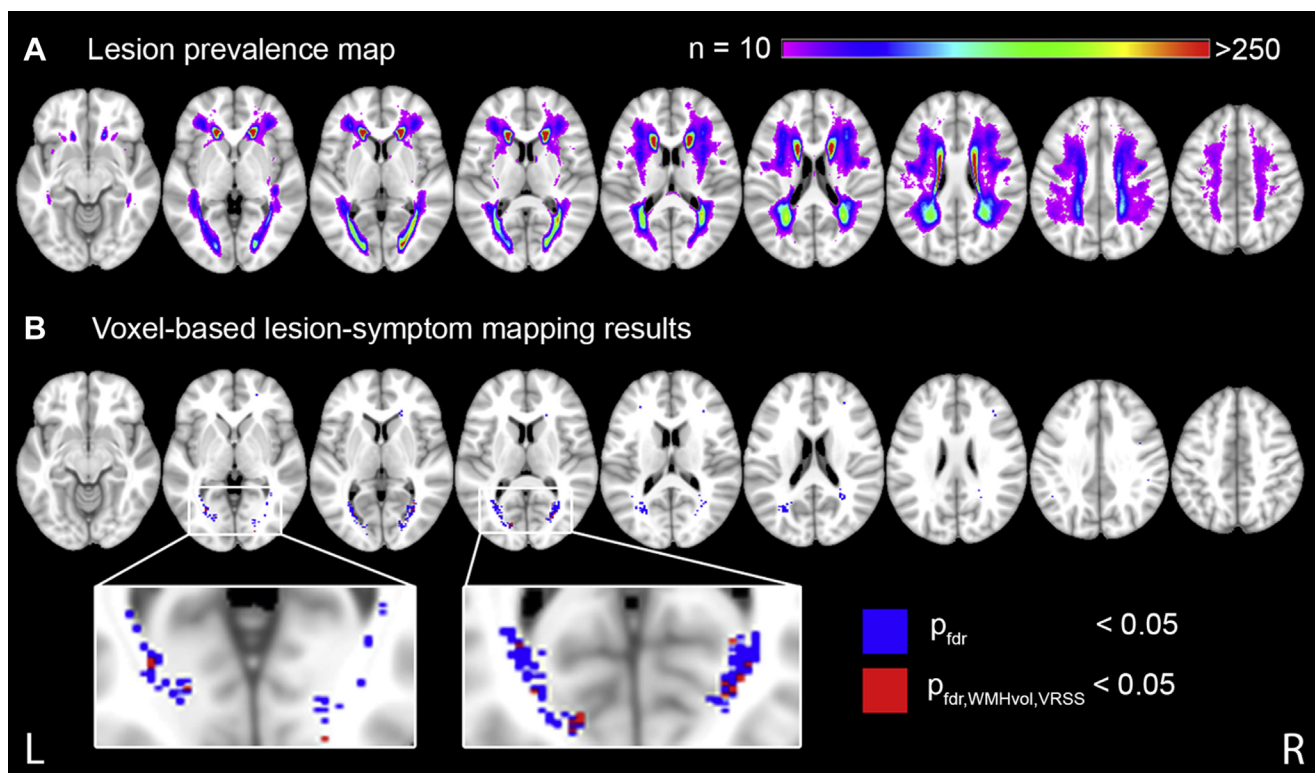


Fig. 2. Lesion prevalence map and voxel-based lesion-symptom mapping results. (A) Lesion prevalence map of WMH in the study sample, shown on the Montreal Neurological Institute 152 T1 template (Fonov et al., 2011). The color of each voxel indicates the number of subjects that had WMH in this voxel, ranging from at least 10 (purple) to 250 or more (red). Only voxels that were damaged in at least 10 subjects (2%) are shown here because this was the minimum threshold for inclusion in the voxel-based lesion-symptom mapping analyses (see Fig. 2B). (B) Voxel-based lesion-symptom mapping results for the relationship with lowered amyloid-beta levels, shown in the axial plane. Voxels damaged in at least 10 subjects (2%) were included in the analyses, as shown in Fig. 2A. Significant voxels after correction for multiple comparisons, age and sex are depicted in blue; significant voxels after additional correction for normalized total WMH volume and the vascular risk summary score are depicted in red (nonparametric mapping settings: Brunner Munzel test; FDR threshold: $q < 0.05$). Nonsignificant voxels are not shown. The right hemisphere is shown on the right. Z-coordinates (axial plane): 63, 73, 78, 83, 88, 93, 98, 108, and 118. Abbreviations: FDR, false discovery rate; L, left; R, right; VRSS, vascular risk summary score; WMH, white matter hyperintensity. (For interpretation of the references to color in this figure legend, the reader is referred to the Web version of this article.)

Table 2

Region of interest-based analyses: cerebrospinal fluid amyloid-beta 1–42 levels or presence of abnormality in relation to regional WMH volumes

Regional WMH volumes	Model 1: age + sex		Model 2: model 1 + CSF Aβ-42 levels		Model 3: model 1 + CSF Aβ-42 abnormality (<640 ng/L)	
	Adj R2		Adj R2	Stdβ	Adj R2	Stdβ
Total	0.143		0.157	-0.131^a	0.147	-0.080
Genu corpus callosum	0.122		0.124	-0.065	0.121	-0.035
Body corpus callosum	0.138		0.138	-0.050	0.136	-0.015
Splenium corpus callosum	0.141		0.170	-0.180^a	0.157	-0.136^a
Anterior limb internal capsule	0.096		0.096	0.044	0.099	0.067
Posterior limb internal capsule	0.067		0.072	0.085	0.074	0.095
Retrolenticular limb internal capsule	0.056		0.055	-0.031	0.054	-0.006
Anterior corona radiata	0.149		0.154	-0.082	0.149	-0.043
Superior corona radiata	0.137		0.138	-0.051	0.136	-0.012
Posterior corona radiata	0.126		0.135	-0.108	0.128	-0.061
Posterior thalamic radiation	0.113		0.142	-0.180^a	0.129	-0.135^a
Sagittal striatum	0.059		0.069	-0.108	0.062	-0.073
External capsule	0.098		0.101	0.066	0.105	0.094
Superior longitudinal fasciculus	0.091		0.094	-0.071	0.089	-0.019
Superior fronto-occipital fasciculus	0.086		0.085	0.002	0.085	0.014
Tapetum	0.087		0.091	-0.076	0.089	-0.035

This linear regression analysis served to identify strategic white matter regions in which CSF Aβ-42 levels or abnormality are associated with regional WMH volumes. The ICBM DTI-81 white matter atlas (Mori et al., 2008; Oishi et al., 2008) was used to calculate regional WMH volumes (in milliliters) for each subject. Bilateral white matter regions were merged to create a single ROI by combining the volumes of the left and right ROI. WMH volumes underwent cube root transformation before statistical analyses. First, age and sex were entered as independent variables into a linear regression model for each ROI (model 1). Next, Aβ-42 was added as continuous measure of CSF levels (model 2), or as dichotomous measure using <640 ng/L as cutoff for abnormal Aβ-42 (model 3). Explained variances (Adj R2) and standardized betas are shown for both measures of CSF Aβ-42. For model 3, standardized betas are multiplied by -1, so negative values correspond with higher WMH volumes being related to abnormal CSF Aβ-42, to allow for better comparison with model 2.

Key: Adj R2, adjusted R2; Aβ-42, amyloid-beta 1–42; CSF, cerebrospinal fluid; ROI, region of interest; Stdβ, standardized beta; WMH, white matter hyperintensity.

^a Statistically significant after Bonferroni correction for 16 comparisons (i.e., $p < 0.0031$), shown in bold.

at <640 ng/L) were both associated with larger WMH volumes in the splenium of the corpus callosum ($\text{std}\beta = -0.180, p < 0.001$; $\text{std}\beta = -0.136, p = 0.001$, respectively) and the posterior thalamic radiation ($\text{std}\beta = -0.180, p < 0.001$; $\text{std}\beta = -0.135, p = 0.001$, respectively), after correction for age and sex (Table 2; Supplementary Fig. 1). The observed associations were independent of clinical diagnosis (interaction terms all nonsignificant). Results remained unchanged after additional correction for the vascular risk summary score and the presence of strictly lobar microbleeds

(Supplementary Table 3). Individual vascular risk factors also did not affect these associations (data not shown). In the subgroup with biologically defined AD (i.e., amyloid- and tau-positive), associations between CSF Aβ-42 levels and WMH volume were similar in these ROIs (splenium: $\text{std}\beta = -0.178, p = 0.007$; posterior thalamic radiation: $\text{std}\beta = -0.253, p < 0.001$). Two additional parieto-occipital white matter ROIs also showed significant associations in this subgroup analysis, namely the sagittal striatum and superior longitudinal fasciculus (Supplementary Table 4).

Table 3

Region of interest-based analyses: cerebrospinal fluid phosphorylated tau levels or presence of abnormality in relation to regional WMH volumes

Regional WMH volumes	Model 1: age + sex		Model 2: model 1 + CSF p-tau levels		Model 3: model 1 + CSF p-tau abnormality (>52 ng/L)	
	Adj R2		Adj R2	Stdβ	Adj R2	Stdβ
Total	0.143		0.144	-0.059	0.142	-0.021
Genu corpus callosum	0.122		0.121	-0.033	0.121	-0.022
Body corpus callosum	0.138		0.144	-0.094	0.138	-0.042
Splenium corpus callosum	0.141		0.140	-0.018	0.140	-0.006
Anterior limb internal capsule	0.096		0.113	-0.140^a	0.100	-0.073
Posterior limb internal capsule	0.067		0.086	-0.148^a	0.073	-0.088
Retrolenticular limb internal capsule	0.056		0.058	-0.065	0.056	-0.045
Anterior corona radiata	0.149		0.152	-0.068	0.148	-0.011
Superior corona radiata	0.137		0.153	-0.134^a	0.140	-0.069
Posterior corona radiata	0.126		0.132	-0.087	0.129	-0.073
Posterior thalamic radiation	0.113		0.113	0.046	0.112	0.029
Sagittal striatum	0.059		0.057	0.008	0.057	0.010
External capsule	0.098		0.114	-0.137^a	0.099	-0.053
Superior longitudinal fasciculus	0.091		0.095	-0.079	0.091	-0.039
Superior fronto-occipital fasciculus	0.086		0.105	-0.146^a	0.090	-0.075
Tapetum	0.087		0.085	0.008	0.085	-0.007

This linear regression analysis served to identify strategic white matter regions in which CSF p-tau levels or abnormality are associated with regional WMH volumes. The ICBM DTI-81 white matter atlas (Mori et al., 2008; Oishi et al., 2008) was used to calculate regional WMH volumes (in milliliters) for each subject. Bilateral white matter regions were merged to create a single ROI by combining the volumes of the left and right ROI. WMH volumes underwent cube root transformation before statistical analyses. First, age and sex were entered as independent variables into a linear regression model for each ROI (model 1). Next, p-tau was added as a continuous measure of CSF levels (model 2), or as dichotomous measure using >52 ng/L as cutoff for abnormal p-tau (model 3). Explained variances (Adj R2) and standardized betas are shown for both measures of CSF p-tau. For model 3, standardized betas are multiplied by -1, so negative values correspond with higher WMH volumes being related to abnormal CSF p-tau, to allow for better comparison with model 2.

Key: Adj R2, adjusted R2; CSF, cerebrospinal fluid; p-tau, phosphorylated tau at threonine 181; ROI, region of interest; Stdβ, standardized beta; WMH, white matter hyperintensity.

^a Statistically significant after Bonferroni correction for 16 comparisons (i.e., $p < 0.0031$), shown in bold.

3.4. Relation between p-tau and WMHs

Overall, CSF p-tau levels were not associated with total WMH volume (**Table 3**). In VLSM, CSF p-tau levels showed no voxelwise correlations with WMH location after correction for sex, age, and multiple comparisons.

In the ROI-based analyses, lower CSF p-tau levels (continuous measure) were associated with larger WMH volumes in fronto-parietal regions, including the internal and external capsule, superior corona radiata, and superior fronto-occipital fasciculus. An interaction between CSF p-tau levels and clinical disease severity was found for WMHs in the posterior limb of the internal capsule; diagnostic subgroup analysis showed that these associations were driven by patients with MCI (std β for SCD: -0.002; MCI: -0.319; AD dementia: 0.019; other dementia: -0.006). By contrast, the presence of CSF p-tau abnormality (dichotomous at >52 ng/L) showed no associations with regional WMH volumes (**Table 3**). In the subgroup with biologically defined AD, no significant associations between CSF p-tau levels and regional WMH volumes were observed (**Supplementary Table 4**).

4. Discussion

We found that lower CSF A β -42 levels are related to WMHs located in the splenium of the corpus callosum and the posterior thalamic radiation in memory clinic patients, also after controlling for markers of vascular disease. This suggests that increased cerebral amyloid burden is linked to WMH occurrence in specific posterior white matter regions.

Previous studies already found indications for a posterior predominance of WMHs in patients with AD as a clinical or genetic diagnosis. One study found that patients with a clinical diagnosis of AD—without information on CSF biomarkers—had significantly higher WMH volumes in posterior periventricular regions and the splenium of the corpus callosum than cognitively normal individuals (Yoshita et al., 2006). Another study showed that WMHs in parietal and occipital lobes are a very early finding in autosomal-dominant AD mutation carriers, occurring more than two decades before symptom onset (Lee et al., 2016). In recent years, a more direct link between cerebral amyloid burden and global WMH burden was suggested by observations in various patient populations (Kandel et al., 2016; Marnane et al., 2016; Osborn et al., 2018; Pietroboni et al., 2018; Scott et al., 2016; Shams et al., 2016; Van Westen et al., 2016). Taking this emerging evidence together, we hypothesized that the burden cerebral amyloid pathology—particularly in the context of clinical AD—contributes to WMHs in posterior brain regions. One recent study indeed found a relationship between lower CSF A β -42 levels and WMHs located in the posterior corona radiata using voxel-based analyses, in subjects with normal cognition or MCI (Al-Janabi et al., 2018). However, this study had a small sample size (n = 62) and did not include individuals with dementia. In addition, the analyses in this study were not corrected for total WMH burden or markers of vascular disease. With this large-scale lesion-mapping study in 517 memory clinic patients, we have now established a direct relationship between the actual cerebral amyloid burden and WMH location in specific posterior brain regions. Furthermore, we have determined that this link between amyloid burden and posterior WMH is present across the full spectrum of clinical disease stages and pathologies that is seen at the memory clinic, and also applies specifically to patients with biologically defined AD.

The observed relationship between lower CSF A β -42 levels and posterior WMHs in specific white matter regions may suggest an amyloidogenic source of white matter damage. Although our study was not designed to establish causality, we speculate that this could

arise through two potential pathways. First, our findings could represent an interaction between cerebral SVD, as manifested in an increased WMH burden, and amyloid pathology, in line with the two-hit vascular hypothesis of AD (Kisler et al., 2017). This hypothesis states that vascular damage leads to accumulation of cerebral amyloid, which in turn causes further damage to small arteries and arterioles. CAA is considered to be one of the key manifestations of this process. CAA is present in over 90% of patients with AD (Esiri et al., 2015), CSF A β -42 is decreased to similar extent in both CAA and AD (Charidimou et al., 2018) and CAA vascular pathology is most abundant in blood vessels located in posterior brain regions (Esiri et al., 2015; Reijmer et al., 2016). Thus the occurrence of posterior WMHs could be related to CAA-related ischemic damage. However, this is challenged by our observation that associations between CSF A β -42 levels and posterior WMH volumes were independent from the presence of strictly lobar cerebral microbleeds, which is a key imaging marker for CAA (Linn et al., 2010). Alternatively, WMHs could be related to direct effects of amyloid pathology on the white matter. We found that the associations between CSF A β -42 and WMH were independent of a vascular risk summary score (representing risk of arteriosclerosis), which agrees with a recent report on patients with autosomal-dominant AD (Lee et al., 2016). Recent evidence suggests that WMHs have heterogeneous features and could represent different underlying pathological processes, particularly in the context of AD pathology (Brickman et al., 2009; Wardlaw et al., 2015). Notably, a postmortem study found that parietal white matter lesions (i.e., the histological equivalent of WMHs) were associated with pathological markers of Wallerian neurodegeneration in patients with AD, whereas ischemic changes related to hypoperfusion were selectively found in nondemented controls. In this same study, neurodegenerative markers were associated with increased burden of cortical AD pathology, but not with SVD-related ischemia (McAleese et al., 2017). This suggests that parietal WMHs may have a distinct pathological composition in the context of AD pathology. Whether these neurodegenerative effects are directly related to amyloid pathology, and whether these changes are region-specific, remain to be determined.

Our findings contribute to a growing body of evidence that proposes that SVD and AD pathologies drive progression to dementia through regionally distinct pathways. This hypothesis states that frontal white matter is preferentially vulnerable to arteriosclerosis-related SVD, whereas posterior white matter changes are more related to neurodegenerative diseases (Kalaria and Ihara, 2013). WMHs appear to follow this spatial distribution: WMHs have an anterior distribution in patients with cerebral autosomal dominant arteriopathy with subcortical infarcts and leukoencephalopathy (Auer et al., 2001; Singhal et al., 2005), and a posterior distribution in patients with clinical AD (Lee et al., 2016; Yoshita et al., 2006). From a clinical perspective, it is relevant to establish whether WMH features can help distinguish between underlying etiologies. Although the stand-alone value of WMH distribution appears to be limited (R² for CSF A β -42 is 3%), it is conceivable that other WMH features might provide additional information. For example, a recent study presented a WMH shape features algorithm, which could be used to compare WMH shapes and sizes in patients with and without amyloid abnormality (De Bresser et al., 2018).

Our secondary objective was to explore the relation between CSF p-tau and WMH location. We found that lower CSF p-tau levels were associated with larger regional WMH volumes, but no associations were found when cutoff scores for CSF abnormality was used. Previous studies on associations between WMH burden and CSF p-tau are scarce and provide conflicting results. One study found that patients with prodromal AD and normal CSF p-tau levels (cutoff for

abnormality: >51 ng/L) had higher parietal WMH burden (Hertz et al., 2013). By contrast, another study found that cognitive normal individuals and patients with MCI who had increased CSF p-tau levels (>23 ng/L) showed more extensive occipital periventricular WMH (NB: graded with a semiquantitative visual rating scale, not WMH volume) (Marnane et al., 2016). Our inconclusive findings in the present study could result from the issue that CSF p-tau levels, as continuous measure, do not necessarily reflect tau pathology burden in the brain. While some neuropathological studies showed a relation between higher CSF p-tau levels and cortical tau pathology (Buerger et al., 2006; Tapiola et al., 2009), these are contested by an equal number of negative studies (Buerger et al., 2007; Engelborghs et al., 2007). Therefore the findings for CSF p-tau levels (i.e., model 2) should be interpreted with caution, and the presence of p-tau pathology should be primarily based on the validated cutoff scores for CSF p-tau abnormality (i.e., model 3). Thus, no clear evidence for any association between CSF p-tau and WMH location was found. PET-tau measures might be more suitable to represent cerebral tau pathology.

Some limitations to our study must also be noted. First, our cross-sectional design does not allow us to make formal causal inferences on the relationship between CSF biomarkers and WMHs. Second, our memory clinic population was included from tertiary referral centers, and participants were only included if they had a minimal burden of vascular brain injury on MRI. This could cause selection bias toward different pathologies than would be seen in regular memory clinics, which could limit the generalizability of our findings. Further studies in other cohorts are therefore recommended. Third, although we achieved much better brain coverage than in previous studies, it should be taken into account that the ROI-based analyses results are based on only parts of each ROI (Supplementary Table 2). For example, although WMHs in the splenium of the corpus callosum were significantly associated with lower CSF A β -42, WMHs were only present in the periventricular parts of this ROI (as seen in Fig. 2A and Supplementary Fig. 1). Fourth, the potential relevance of other A β species was not addressed. A previous study found that decreased CSF A β -38 and A β -40 levels, indicative of A β deposition in the cerebral vessel walls, were more strongly associated with regional WMHs than CSF A β -42 (Van Westen et al., 2016). This could be relevant in the context of CAA (Charidimou et al., 2018) and warrants further investigation. Fifth, MRI data were collected from various scanner types and imaging protocols. We accounted for this by using a WMH segmentation algorithm and image-processing pipeline that were validated for different types imaging data, but this remains a potential source of heterogeneity. Finally, CSF biomarkers cannot provide information on the location of amyloid or tau abnormalities in the brain. Studies on positron emission tomography imaging of amyloid and tau could help determine whether posterior WMHs colocalize with AD pathology.

In conclusion, our findings indicate that cerebral amyloid burden is associated with WMHs located in specific posterior white matter regions, possibly reflecting region-specific effects of amyloid pathology on the white matter. CSF-pathological-imaging studies are necessary to further establish the pathways that link amyloid pathology to WMHs.

Disclosure

The TRACE-VCI study is supported by Vidi grant 917.11.384 and Vici Grant 918.16.616 from ZonMw (The Netherlands Organisation for Health Research and Development), and grant 2010T073 from the Dutch Heart Association to Geert Jan Biessels.

Alzheimer Center Amsterdam research is part of the neurodegeneration research program of the Amsterdam Neuroscience. Alzheimer Center Amsterdam is supported by Stichting Alzheimer

Nederland and Stichting VUMC funds. The clinical database structure was developed with funding from Stichting Dioraphte. Wiesje van der Flier holds the Pasman chair. Frederik Barkhof is supported by the NIHR biomedical research center at UCLH.

There are no declarations of interest related to this article.

Acknowledgements

Members of the TRACE-VCI study group supporting the present study (in alphabetical order, per department): *VU University Medical Centre, Amsterdam, the Netherlands:* Alzheimer Centre and Department of neurology: M.R. Benedictus, J. Bremer, W.M. van der Flier, J. Leijenaar, N.D. Prins, P. Scheltens, B.M. Tijms. Department of Radiology and Nuclear Medicine: F. Barkhof, M.P. Wattjes. Department of Clinical Chemistry: C.E. Teunissen. Department of Medical Psychology: T. Koene. *University Medical Centre Utrecht, Utrecht, the Netherlands:* Department of Neurology: E. van den Berg, H. van den Brink, G.J. Biessels, L.G. Exalto, D.A. Ferro, O. Groeneveld, R. Heinen, S.M. Heringa, L.J. Kappelle, Y.D. Reijmer, J. Verwer. Department of Radiology/Image Sciences Institute: J. de Bresser, H.J. Kuijf. Department of Geriatrics: H.L. Koek. *Hospital Diaconessenhuis Zeist, the Netherlands:* M. Hamaker, R. Faaij, M. Pleizier, E. Vriens. *Onze Lieve Vrouwe Gasthuis (OLVG) West, Amsterdam, the Netherlands:* Department of Neurology: J.M.F. Boomsma, H.M. Boss, H.C. Weinstein.

The authors greatly acknowledge the use of MeVisLab.

Appendix A. Supplementary data

Supplementary data to this article can be found online at <https://doi.org/10.1016/j.neurobiolaging.2019.08.001>.

References

- Al-Janabi, O.M., Brown, C.A., Bahrani, A.A., Abner, E.L., Barber, J.M., Gold, B.T., Goldstein, L.B., Murphy, R.R., Nelson, P.T., Johnson, N.F., Shaw, L.M., Smith, C.D., Trojanowski, J.Q., Wilcock, D.M., Jicha, G.A., 2018. Distinct white matter changes associated with cerebrospinal fluid amyloid- β 1-42 and hypertension. *J. Alzheimers Dis.* 66, 1095–1104.
- Auer, D.P., Pütz, B., Gössl, C., Elbel, G.-K., Gasser, T., Dichgans, M., 2001. Differential lesion patterns in CADASIL and sporadic subcortical Arteriosclerotic Encephalopathy: MR imaging study with statistical parametric group comparison. *Radiology* 218, 443–451.
- Blennow, K., Hampel, H., Weiner, M., Zetterberg, H., 2010. Cerebrospinal fluid and plasma biomarkers in Alzheimer disease. *Nat. Rev. Neurol.* 6, 131–144.
- Blennow, K., Mattsson, N., Schöll, M., Hansson, O., Zetterberg, H., 2015. Amyloid biomarkers in Alzheimer's disease. *Trends Pharmacol. Sci.* 36, 297–309.
- Boomsma, J.M.F., Exalto, L.G., Barkhof, F., van den Berg, E., de Bresser, J., Heinen, R., Koek, H.L., Prins, N.D., Scheltens, P., Weinstein, H.C., van der Flier, W.M., Biessels, G.J., 2017. Vascular cognitive impairment in a memory clinic population: Rationale and design of the "Utrecht-Amsterdam clinical features and prognosis in vascular cognitive impairment" (TRACE-VCI) study. *JMIR Res. Protoc.* 6, e60.
- Brickman, A.M., 2013. Contemplating alzheimer's disease and the contribution of white matter hyperintensities. *Curr. Neurol. Neurosci. Rep.* 13, 415.
- Brickman, A.M., Muraskin, J., Zimmerman, M.E., 2009. Structural neuroimaging in Alzheimer's disease: do white matter hyperintensities matter? *Dialogues Clin. Neurosci.* 11, 181–190.
- Brickman, A.M., Provenzano, F.A., Muraskin, J., Manly, J.J., Blum, S., Apa, Z., Stern, Y., Brown, T.R., Luchsinger, J.A., Mayeux, R., 2012. Regional white matter hyperintensity volume, not hippocampal atrophy, predicts incident Alzheimer disease in the community. *Arch. Neurol.* 69, 1621–1627.
- Buerger, K., Ewers, M., Pirttilä, T., Zinkowski, R., Alafuzoff, I., Teipel, S.J., DeBernardis, J., Kerkman, D., McCulloch, C., Soininen, H., Hampel, H., 2006. CSF phosphorylated tau protein correlates with neocortical neurofibrillary pathology in Alzheimer's disease. *Brain* 129, 3035–3041.
- Buerger, K., Alafuzoff, I., Ewers, M., Pirttilä, T., Zinkowski, R., Hampel, H., 2007. No correlation between CSF tau protein phosphorylated at threonine 181 with neocortical neurofibrillary pathology in Alzheimer's disease. *Brain* 130, e82.
- Chao, C.P., Kotzenas, A.L., Broderick, D.F., 2006. Cerebral amyloid angiopathy: CT and MR imaging findings. *RadioGraphics* 26, 1517–1531.
- Charidimou, A., Friedrich, J.O., Greenberg, S.M., Viswanathan, A., 2018. Core cerebrospinal fluid biomarker profile in cerebral amyloid angiopathy. *Neurology* 90, e754–e762.
- De Bresser, J., Kuijf, H.J., Zaanen, K., Viergever, M.A., Hendrikse, J., Biessels, G.J., Algra, A., Van Den Berg, E., Bouvy, W., Brundel, M., Heringa, S., Kappelle, L.J.,

- Leemans, A., Luijten, P.R., Mali, W.P.T.M., Rutten, G.E.H.M., Vincken, K.L., Zwanenburg, J., 2018. White matter hyperintensity shape and location feature analysis on brain MRI: Proof of principle study in patients with diabetes. *Sci. Rep.* 8, 1–10.
- de Haan, B., Karnath, H.O., 2017. A hitchhiker's guide to lesion-behaviour mapping. *Neuropsychologia* 115, 5–16.
- Engelborghs, S., Sleegers, K., Cras, P., Brouwers, N., Serneels, S., De Leenheer, E., Martin, J.J., Vanmechelen, E., Van Broeckhoven, C., De Deyn, P.P., 2007. No association of CSF biomarkers with APOE4, plaque and tangle burden in definite Alzheimer's disease. *Brain* 130, 2320–2326.
- Esiri, M., Chance, S., Joachim, C., Warden, D., Smallwood, A., Sloan, C., Christie, S., Wilcock, G., Smith, A.D., 2015. Cerebral amyloid angiopathy, subcortical white matter disease and dementia: Literature review and study in OPTIMA. *Brain Pathol.* 25, 51–62.
- Fonov, V., Evans, A.C., Botteron, K., Almli, C.R., McKinstry, R.C., Collins, D.L., Brain Development Cooperative Group, 2011. Unbiased average age-appropriate atlases for pediatric studies. *Neuroimage* 54, 313–327.
- Gorelick, P.B., Scuteri, A., Black, S.E., Decarli, C., Greenberg, S.M., Iadecola, C., Launer, L.J., Laurent, S., Lopez, O.L., Nyenhuis, D., Petersen, R.C., Schneider, J.A., Tzourio, C., Arnett, D.K., Bennett, D.A., Chui, H.C., Higashida, R.T., Lindquist, R., Nilsson, P.M., Roman, G.C., Sellke, F.W., Seshadri, S., 2011. Vascular contributions to cognitive impairment and dementia: a statement for healthcare professionals from the American Heart Association/American Stroke Association. *Stroke* 42, 2672–2713.
- Hertz, J., Palmqvist, S., Minthon, L., Hansson, O., 2013. Tau pathology and parietal white matter lesions have independent but synergistic effects on early development of Alzheimer's disease. *Dement. Geriatr. Cogn. Dis. Extra* 3, 113–122.
- Jack, C.R., Bennett, D.A., Blennow, K., Carrillo, M.C., Dunn, B., Haeberlein, S.B., Holtzman, D.M., Jagust, W., Jessen, F., Karlawish, J., Liu, E., Molinuevo, J.L., Montine, T., Phelps, C., Rankin, K.P., Rowe, C.C., Scheltens, P., Siemers, E., Snyder, H.M., Sperling, R., Elliott, C., Masliah, E., Ryan, L., Silverberg, N., 2018. NIA-AA Research Framework: toward a biological definition of Alzheimer's disease. *Alzheimer's Dement.* 14, 535–562.
- Kalaria, R.N., 2000. The role of cerebral ischemia in Alzheimer's disease. *Neurobiol Aging* 21, 321–330.
- Kalaria, R.N., Ihara, M., 2013. Dementia: vascular and neurodegenerative pathways – will they meet? *Nat. Rev. Neurol.* 9, 487–488.
- Kandel, B.M., Avants, B.B., Gee, J.C., McMillan, C.T., Erus, G., Doshi, J., Davatzikos, C., Wolk, D.A., 2016. White matter hyperintensities are more highly associated with preclinical Alzheimer's disease than imaging and cognitive markers of neurodegeneration. *Alzheimers Dement. Diagnosis, Assess. Dis. Monit.* 4, 18–27.
- Kisler, K., Nelson, A.R., Montagne, A., Zlokovic, B.V., 2017. Cerebral blood flow regulation and neurovascular dysfunction in Alzheimer disease. *Nat. Rev. Neurosci.* 18, 419–434.
- Klein, S., Staring, M., Murphy, K., Viergever, M.A., Pluim, J.P.W., 2010. Elastix: a toolbox for intensity-based medical image registration. *IEEE Trans. Med. Imaging* 29, 196–205.
- Koncz, R., Sachdev, P.S., 2018. Are the brain's vascular and Alzheimer pathologies additive or interactive? *Curr. Opin. Psychiatry* 31, 147–152.
- Lee, S., Viqar, F., Zimmerman, M.E., Narkhede, A., Tosto, G., Benzinger, T.L.S., Marcus, D.S., Fagan, A.M., Goate, A., Fox, N.C., Cairns, N.J., Holtzman, D.M., Buckles, V., Ghetti, B., McDade, E., Martins, R.N., Saykin, A.J., Masters, C.L., Ringman, J.M., Ryan, N.S., Förster, S., Laske, C., Schofield, P.R., Sperling, R.A., Salloway, S., Correia, S., Jack, C., Weiner, M., Bateman, R.J., Morris, J.C., Mayeux, R., Brickman, A.M., 2016. White matter hyperintensities are a core feature of Alzheimer's disease: evidence from the dominantly inherited Alzheimer network. *Ann. Neurol.* 79, 929–939.
- Lewczuk, P., Kornhuber, J., Wiltfang, J., 2006. The German Competence Net Dementias: standard operating procedures for the neurochemical dementia diagnostics. *J. Neural Transm.* 113, 1075–1080.
- Lindemer, E.R., Salat, D.H., Smith, E.E., Nguyen, K., Fischl, B., Greve, D.N., Alzheimer's Disease Neuroimaging Initiative, 2015. White matter signal abnormality quality differentiates MCI that Converts to Alzheimer's disease from non-converters HHS public access. *Neurobiol. Aging* 36, 2447–2457.
- Linn, J., Halpin, A., Demaerel, P., Ruhland, J., Giese, A.D., Dichgans, M., van Buchem, M.A., Bruckmann, H., Greenberg, S.M., 2010. Prevalence of superficial siderosis in patients with cerebral amyloid angiopathy. *Neurology* 74, 1346–1350.
- Marnane, M., Al-Jawadi, O.O., Mortazavi, S., Pogorzelec, K.J., Wang, B.W., Feldman, H.H., Hsiung, G.Y.R., 2016. Periventricular hyperintensities are associated with elevated cerebral amyloid. *Neurology* 86, 535–543.
- McAleese, K.E., Walker, L., Graham, S., Moya, E.L.J., Johnson, M., Erskine, D., Colloby, S.J., Dey, M., Martin-Ruiz, C., Taylor, J.P., Thomas, A.J., McKeith, I.G., De Carli, C., Attrens, J., 2017. Parietal white matter lesions in Alzheimer's disease are associated with cortical neurodegenerative pathology, but not with small vessel disease. *Acta Neuropathol.* 134, 459–473.
- Molinuevo, J.L., Ayton, S., Batrla, R., Bednar, M.M., Bittner, T., Cummings, J., Fagan, A.M., Hampel, H., Mielke, M.M., Mikulskis, A., O'Bryant, S., Scheltens, P., Sevigny, J., Shaw, L.M., Soares, H.D., Tong, G., Trojanowski, J.Q., Zetterberg, H., Blennow, K., 2018. Current State of Alzheimer's Fluid Biomarkers. *Acta Neuropathologica* 136, 821–853.
- Mori, S., Oishi, K., Jiang, H., Jiang, L., Li, X., Akhter, K., Hua, K., Faria, A.V., Mahmood, A., Woods, R., Toga, A.W., Pike, G.B., Neto, P.R., Evans, A., Zhang, J., Huang, H., Miller, M.I., van Zijl, P., Mazziotta, J., 2008. Stereotaxic white matter atlas based on diffusion tensor imaging in an ICBM template. *Neuroimage* 40, 570–582.
- Mulder, C., Verwey, N.A., Van Der Flier, W.M., Bouwman, F.H., Kok, A., Van Elk, E.J., Scheltens, P., Blankenstein, M.A., 2010. Amyloid- β (1–42), total tau, and phosphorylated tau as cerebrospinal fluid biomarkers for the diagnosis of Alzheimer disease. *Clin. Chem.* 56, 248–253.
- O'Brien, J.T., Erkinjuntti, T., Reisberg, B., Roman, G., Sawada, T., Pantoni, L., Bowler, J.V., Ballard, C., DeCarli, C., Gorelick, P.B., Rockwood, K., Burns, A., Gauthier, S., DeKosky, S.T., 2003. Vascular cognitive impairment. *Lancet Neurol.* 2, 89–98.
- Oishi, K., Zilles, K., Amunts, K., Faria, A., Jiang, H., Li, X., Akhter, K., Hua, K., Woods, R., Toga, A.W., Pike, G.B., Rosa-Neto, P., Evans, A., Zhang, J., Huang, H., Miller, M.I., van Zijl, P.C.M., Mazziotta, J., Mori, S., 2008. Human brain white matter atlas: Identification and assignment of common anatomical structures in superficial white matter. *Neuroimage* 43, 447–457.
- Osborn, K.E., Liu, D., Samuels, L.R., Moore, E.E., Cambronero, F.E., Acosta, L.M.Y., Bell, S.P., Babicz, M.A., Gordon, E.A., Pechman, K.R., Davis, L.T., Gifford, K.A., Hohman, T.J., Blennow, K., Zetterberg, H., Jefferson, A.L., 2018. Cerebrospinal fluid β -amyloid42 and neurofilament light relate to white matter hyperintensities. *Neurobiol. Aging* 68, 18–25.
- Pantoni, L., 2010. Cerebral small vessel disease: from pathogenesis and clinical characteristics to therapeutic challenges. *Lancet Neurol.* 9, 689–701.
- Pietroboni, A.M., Scarioni, M., Carandini, T., Basilico, P., Cadioli, M., Giulietti, G., Arighi, A., Caprioli, M., Serra, L., Sina, C., Fenoglio, C., Ghezzi, L., Fumagalli, G.G., De Riz, M.A., Calvi, A., Triulzi, F., Bozzali, M., Scarpini, E., Galimberti, D., 2018. CSF β -amyloid and white matter damage: a new perspective on Alzheimer's disease. *J. Neurol. Neurosurg. Psychiatry* 89, 352–357.
- Prins, N.D., Van Dijk, E.J., Den Heijer, T., Vermeer, S.E., Koudstaal, P.J., Oudkerk, M., Hofman, A., Breteler, M.M.B., 2004. Cerebral white matter lesions and the risk of dementia. *Arch. Neurol.* 61, 1531–1534.
- Reijmer, Y.D., van Veluw, S.J., Greenberg, S.M., 2016. Ischemic brain injury in cerebral amyloid angiopathy. *J. Cereb. Blood Flow Metab.* 36, 40–54.
- Rezek, D.L., Morris, J.C., Fulling, K.H., Gado, M.H., 1987. Periventricular white matter lucencies in senile dementia of the Alzheimer type and in normal aging. *Neurology* 37, 1365–1368.
- Ritter, F., Boskamp, T., Homeyer, A., Laue, H., Schwier, M., Link, F., Peitgen, H., 2011. Medical image analysis. *IEEE Pulse* 2, 60–70.
- Rorden, C., Karnath, H.O., Bonilha, L., 2007. Improving lesion-symptom mapping. *J. Cogn. Neurosci.* 19, 1081–1088.
- Rorden, C., Bonilha, L., Fridriksson, J., Bender, B., Karnath, H.-O., 2012. Age-specific CT and MRI templates for spatial normalization. *Neuroimage* 61, 957–965.
- Ryan, N.S., Biessels, G.-J., Kim, L., Nicholas, J.M., Barber, P.A., Walsh, P., Gami, P., Morris, H.R., Bastos-Leite, A.J., Schott, J.M., Beck, J., Mead, S., Chavez-Gutierrez, L., de Strooper, B., Rossor, M.N., Revesz, T., Lashley, T., Fox, N.C., 2015. Genetic determinants of white matter hyperintensities and amyloid angiopathy in familial Alzheimer's disease. *Neurobiol. Aging* 36, 3140–3151.
- Scheltens, P.H., Barkhof, F., Valk, J., Algra, P.R., van der Hoop, R.G., Nauta, J., Wolters, E.C., 1992. White matter lesions on magnetic resonance imaging in clinically diagnosed Alzheimer's disease: evidence for heterogeneity. *Brain* 115, 735–748.
- Scott, J.A., Braskie, M.N., Tosun, D., Maillard, P., Thompson, P.M., Weiner, M., DeCarli, C., Carmichael, O.T., ADNI, 2016. Cerebral amyloid is associated with greater white-matter hyperintensity accrual in cognitively normal older adults. *Neurobiol. Aging* 48, 48–52.
- Shams, S., Granberg, T., Martola, J., Li, X., Shams, M., Fereshtehnejad, S.M., Cavallini, L., Aspelin, P., Kristoffersen-Wiberg, M., Wahlund, L.O., 2016. Cerebrospinal fluid profiles with increasing number of cerebral microbleeds in a continuum of cognitive impairment. *J. Cereb. Blood Flow Metab.* 36, 621–628.
- Singhal, S., Rich, P., Markus, H.S., 2005. The spatial distribution of MR imaging abnormalities in cerebral autosomal dominant arteriopathy with subcortical infarcts and leukoencephalopathy and their relationship to age and clinical features. *Am. J. Neuroradiol.* 26, 2481–2487.
- Smith, E.E., Egorova, S., Blacker, D., Killiany, R.J., Muzikansky, A., Dickerson, B.C., Tanzi, R.E., Albert, M.S., Greenberg, S.M., Guttman, C.R.G., 2008. Magnetic resonance imaging white matter hyperintensities and brain volume in the prediction of mild cognitive impairment and dementia. *Arch. Neurol.* 65, 94–100.
- Steenwijk, M.D., Pouwels, P.J.W., Daams, M., Van Dalen, J.W., Caan, M.W.A., Richard, E., Barkhof, F., Vrenken, H., 2013. Accurate white matter lesion segmentation by k nearest neighbor classification with tissue type priors (kNN-TTPs). *Neuroimage Clin.* 3, 462–469.
- Tapiola, T., Alafuzoff, I., Herukka, S.-K., Parkkinen, L., Hartikainen, P., Soininen, H., Pirttilä, T., 2009. Cerebrospinal fluid β -amyloid 42 and tau proteins as biomarkers of Alzheimer-type pathologic changes in the brain. *Arch. Neurol.* 66, 382–389.
- Thanprasertsuk, S., Martinez-Ramirez, S., Pontes-Neto, O.M., Ni, J., Ayres, A., Reed, A., Swords, K., Gurol, M.E., Greenberg, S.M., Viswanathan, A., 2014. Posterior white matter disease distribution as a predictor of amyloid angiopathy. *Neurology* 83, 794–800.
- Van Westen, D., Lindqvist, D., Blennow, K., Minthon, L., Nägga, K., Stomrud, E., Zetterberg, H., Hansson, O., 2016. Cerebral white matter lesions - associations with $\text{A}\beta$ isoforms and amyloid PET. *Sci. Rep.* 6, 1–9.
- Verhage, F., 1964. Intelligentie en leeftijd: onderzoek bij Nederlanders van twaalf tot zeventien jaar [Intelligence and Age: study with Dutch people aged 12 to 77]. Van Gorcum, Assen.
- Vermeer, S.E., Prins, N.D., den Heijer, T., Hofman, A., Koudstaal, P.J., Breteler, M.M.B., 2003. Silent brain infarcts and the risk of dementia and cognitive decline. *N. Engl. J. Med.* 348, 1215–1222.

- Wardlaw, J.M., Smith, E.E., Biessels, G.J., Cordonnier, C., Fazekas, F., Frayne, R., Lindley, R.I., O'Brien, J.T., Barkhof, F., Benavente, O.R., Black, S.E., Brayne, C., Breteler, M., Chabriat, H., DeCarli, C., de Leeuw, F.E., Doubal, F., Duering, M., Fox, N.C., Greenberg, S., Hachinski, V., Kilimann, I., Mok, V., Oostenbrugge, Rv, Pantoni, L., Speck, O., Stephan, B.C.M., Teipel, S., Viswanathan, A., Werring, D., Chen, C., Smith, C., van Buchem, M., Norrving, B., Gorelick, P.B., Dichgans, M., 2013. Neuroimaging standards for research into small vessel disease and its contribution to ageing and neurodegeneration. *Lancet Neurol.* 12, 822–838.
- Wardlaw, J.M., Valdés Hernández, M.C., Muñoz-Maniega, S., 2015. What are white matter hyperintensities made of? Relevance to vascular cognitive impairment. *J. Am. Heart Assoc.* 4, 001140.
- Weaver, N.A., Zhao, L., Biesbroek, J.M., Kuijf, H.J., Aben, H.P., Bae, H.-J., Caballero, M.Á.A., Chappell, F.M., Chen, C.P.L.H., Dichgans, M., Duering, M., Georgakis, M.K., van der Giessen, R.S., Gyanwali, B., Hamilton, O.K.L., Hilal, S., vom Hofe, E.M., de Kort, P.L.M., Koudstaal, P.J., Lam, B.Y.K., Lim, J.-S., Makin, S.D.J., Mok, V.C.T., Shi, L., Valdés Hernández, M.C., Venketasubramanian, N., Wardlaw, J.M., Wollenweber, F.A., Wong, A., Xin, X., DeCarli, C., Fletcher, E.A., Maillard, P., Barnes, J., Sudre, C.H., Schott, J.M., Ikram, M.A., Papma, J.M., Steketee, R.M.E., Vernooij, M.W., Bordet, R., Lopes, R., Huang, C.-W., Frayne, R., McCreary, C.R., Smith, E.E., Backes, W., Köhler, S., van Oostenbrugge, R.J., Staals, J., Verhey, F., Cheng, C.Y., Kalaria, R.N., Werring, D., Hsu, J.L., Huang, K.-L., van der Grond, J., Jukema, J.W., van der Mast, R.C., Nijboer, T.C.W., Yu, K.-H., Schmidt, R., Pirpamer, L., MacIntosh, B.J., Robertson, A.D., de Leeuw, F.-E., Tuladhar, A.M., Chaturvedi, N., Tillin, T., Brodaty, H., Sachdev, P., Barkhof, F., van der Flier, W.M., Kappelle, L.J., Biessels, G.J., 2019. The Meta VCI Map consortium for meta-analyses on strategic lesion locations for vascular cognitive impairment using lesion-symptom mapping: design and multicenter pilot study. *Alzheimers Dement. Diagnosis, Assess. Dis. Monit.* 11, 310–326.
- Wolf, H., Ecke, G.M., Bettin, S., Dietrich, J., Gertz, H.J., 2000. Do white matter changes contribute to the subsequent development of dementia in patients with mild cognitive impairment? A longitudinal study. *Int. J. Geriatr. Psychiatry* 15, 803–812.
- Yoshita, M., Fletcher, E., Harvey, D., Ortega, M., Martinez, O., Mungas, D.M., Reed, B.R., DeCarli, C.S., 2006. Extent and distribution of white matter hyperintensities in normal aging, MCI, and AD. *Neurology* 67, 2192–2198.
- Zhu, Y.-C., Chabriat, H., Godin, O., Dufouil, C., Rosand, J., Greenberg, S.M., Smith, E.E., Tzourio, C., Viswanathan, A., 2012. Distribution of white matter hyperintensity in cerebral hemorrhage and healthy aging. *J. Neurol.* 259, 530–536.
- Zwan, M., van Harten, A., Ossenkoppele, R., Bouwman, F., Teunissen, C., Adriaanse, S., Lammertsma, A., Scheltens, P., van Berckel, B., van der Flier, W., 2014. Concordance between cerebrospinal fluid biomarkers and [¹¹C]PIB PET in a memory clinic cohort. *J. Alzheimers Dis.* 41, 801–807.